

THE TENNIS RACKET THEOREM, ANALYSIS AND NUMERICAL SIMULATION OF THE INTERMEDIATE AXIS THEOREM

Nicolas Trivisonno¹, Luciano Garelli¹, Mario Storti¹

¹*CIMEC Centro de Investigación de Métodos Computacionales, UNL, CONICET, FICH, Col. Ruta 168 s/n, Predio Conicet "Dr Alberto Cassano", 3000 Santa Fe, Argentina, <http://www.cimec.org.ar>*

Keywords: Tennis racket theorem, Intermediate axis theorem, Dzhanibekov effect, Principal axis instability, Wingnut effect

Abstract. The aim of this paper is to reproduce the phenomenon of the intermediate axes theorem also known as the Dzhanibekov effect or the Tennis Racket effect. A RBD (Rigid Body Dynamic) model with 6DOFs (six degrees of freedom) was developed to reproduce the Euler's law of motion. Furthermore, in the RBD model, quaternions are employed for the mathematical modeling. Then an asymmetrical-top object was analyzed in order to show the intermediate axis effect. Finally, a numerical simulation is performed in order to reproduce the instability.

1 INTRODUCTION

Basically, the intermediate axis theorem also known as tennis racket theorem effect says that in an asymmetrical top object (three different principal inertia moments, where $I_1 < I_2 < I_3$) the spin around the first and third principal inertia is stable, but if the object rounds around the second inertia this motion will perform a weird and periodic movement due to an instability in its spin.

The statement of the intermediate axis theorem has been studied for a long time as it represents a problem for Classical Mechanics, [Poincot \(1851\)](#), [Landau and Lifshitz \(1976\)](#), [Ashbaugh et al. \(1991\)](#). And even reached the category of state secret for some world powers during the space race. It acquires such relevance when the mission Soyuz T-13¹ was realized. Since while the repair to re-activate the space station was being carried out, Commander Dzhanibekov witnessed the mysterious trajectory on a wingnut while performing the maintenance of the equipment, so it is also usually called Dzhanibekov effect or Wingnut effect.

Despite the fact that the intermediate axis theorem is a known concept for long time since it corresponds to the traditional analysis of Classic Mechanics, due to its curious and unusual movement this effect never ceases to amaze anyone who witnesses that mysterious behavior. The aim of this paper is to reproduce this phenomenon through a RBD model that uses quaternions for the mathematical representation. As an indirect profit, reproducing this phenomenon validates the implementation of the RBD model and also proves the potentiality of the quaternions representation since it enables vertical launches, situation that is not possible if the Euler's Angles implementation is used as the singularity known as *gimbal-lack*.

This work consists of a first session in which a classification of objects is presented based on their moments of inertia, [Sec.\(2\)](#). [Sec.\(3\)](#) presents the Rigid Body Dynamic model (RBD) that uses quaternions for the mathematical representation. Then, Euler equations are analyzed for the different object classifications, where the physics of the precessional motion is studied: [Sec.\(4.2\)](#) and [Sec.\(4.3\)](#). Finally, the instability of the intermediate axis is reproduced and analyzed in [Sec.\(6\)](#).

2 DESCRIPTION

Inertia tensor: The inertia of a body is defined by 6 values that constitutes a symmetrical tensor, that means the inertial tensor I is a 2^{nd} order tensor, $I \in CT(2)^2$, [Eq.\(1\)](#). Like all $CT(2)$, this tensor can be transformed to a diagonal tensor if the directions of the axes are correctly chosen, this process is known as diagonalization and the elements of the diagonal are the principal moments of inertia, which corresponds to the inertias in the directions selected to diagonalize the tensor ³.

$$I_{ij} = I_{ji} = \begin{bmatrix} I_{xx} & I_{xy} & I_{xz} \\ I_{xy} & I_{yy} & I_{yk} \\ I_{xz} & I_{yz} & I_{kk} \end{bmatrix} \quad (1)$$

In other words, when the diagonalization of $I \in CT(2)$ is performed, two tensors are obtained: I_d, v , [Eq.\(2\)](#) where $I_d, v \in CT(2)$. I_d is a diagonal tensor, whose diagonal elements

¹It is of note because it marked the first time a spacecraft had docked with a 'dead' space station, and the first time such a station had been returned to operational status following repairs

²CT refers to Cartesian Tensor

³This process is the one carried out when the eigenvalues and eigenvectors of a CT are obtained (2)

are the principal moments of inertia, and the column vectors of the tensor v are the principal directions of inertia.

$$I_d = \begin{bmatrix} I_1 & 0 & 0 \\ 0 & I_2 & 0 \\ 0 & 0 & I_3 \end{bmatrix} v = \begin{bmatrix} v_{11} & v_{21} & v_{31} \\ v_{12} & v_{22} & v_{32} \\ \underbrace{v_{13}}_{v_1} & \underbrace{v_{23}}_{v_2} & \underbrace{v_{33}}_{v_3} \end{bmatrix} \quad (2)$$

Furthermore, by convention, they are organized so that $I_1 > I_2 > I_3$ where these inertias have the particularity that none can exceed the sum of the other two, for example:

$$I_1 + I_2 \geq I_3 \quad (3)$$

The moments of inertia characterize the rotation of a body in a given direction. Depending on how these moments of inertia are, bodies can be classified into different groups:

- all identical inertias: $I_1 = I_2 = I_3$, this object is known as *spherical top*
- two equal inertias and the third not: $I_1 = I_2 \neq I_3$, this object is known as *symmetrical top*
- all different inertias: $I_1 \neq I_2 \neq I_3$, this object is known as *asymmetrical top*

Whenever a body rotates about one of its principal axes, then the moment vector will be aligned with the velocity vector. If the velocity vector (which is given by the ellipsoid of the kinetic energy, KE) stops being collinear with the moment vector, then the motion will change given rise to *precession* phenomenon. Therefore, *precession* can be defined as the parameter that indicates how non-aligned the velocity vector is with respect to the principal axis. In Sec.(4.2) the analysis of the *precession* effect is extended.

3 RBD MODEL - RIGID BODY DYNAMIC MODEL

The RBD (Rigid Body Dynamic) model describes the movement of an object where the governing equation during the trajectory can be classified in kinematics and dynamics. The first one relates linear and angular velocity with the change on position and orientations, the second one relates forces and torques acting on the system with the change on velocity both linear and angular. Kokes et al. (2007) presents the equations of rigid body on the bodyframe Eq.(4,5,6,7) which are valid for any rigid body.

- Cinematics Equations:

$$\begin{bmatrix} \dot{x} \\ \dot{y} \\ \dot{z} \end{bmatrix}_{NED} = \begin{bmatrix} c_\theta c_\psi & s_\phi s_\theta c_\psi - c_\phi s_\psi & c_\phi s_\theta c_\psi + s_\phi s_\psi \\ c_\theta s_\psi & s_\phi s_\theta s_\psi + c_\phi c_\psi & c_\phi s_\theta s_\psi - s_\phi c_\psi \\ -s_\theta & s_\phi c_\theta & c_\phi c_\theta \end{bmatrix} \begin{bmatrix} u \\ v \\ w \end{bmatrix}_{BODY} \quad (4)$$

$$\begin{bmatrix} \dot{\phi} \\ \dot{\theta} \\ \dot{\psi} \end{bmatrix}_{NED} = \begin{bmatrix} 1 & s_\phi t_\theta & c_\phi t_\theta \\ 0 & c_\theta & -s_\phi \\ 0 & s_\phi / c_\theta & c_\phi / c_\theta \end{bmatrix} \begin{bmatrix} p \\ q \\ r \end{bmatrix}_{BODY} \quad (5)$$

- Dynamics Equations:

$$\begin{bmatrix} \dot{u} \\ \dot{v} \\ \dot{w} \end{bmatrix}_{BODY} = \begin{bmatrix} F_x/m \\ F_y/m \\ F_z/m \end{bmatrix}_{BODY} - \begin{bmatrix} 0 & -r & q \\ r & 0 & -p \\ -q & p & 0 \end{bmatrix} \begin{bmatrix} u \\ v \\ w \end{bmatrix}_{BODY} \quad (6)$$

$$\begin{bmatrix} \dot{p} \\ \dot{q} \\ \dot{r} \end{bmatrix}_{BODY} = I^{-1} \left\{ \begin{bmatrix} T_x \\ T_y \\ T_z \end{bmatrix}_{BODY} - \begin{bmatrix} 0 & -r & q \\ r & 0 & -p \\ -q & p & 0 \end{bmatrix} I \begin{bmatrix} p \\ q \\ r \end{bmatrix}_{BODY} \right\} \quad (7)$$

where s_* , c_* and t_* are the usual trigonometric operations ($\cos()$, $\sin()$, $\tan()$), m is the mass of the object, I is the inertial tensor on the body-frame (therefore is constant), $[x, y, z]$ is the position in the inertial frame, and the rest of the vectors are stated in body-frame: $[u, v, w]$ is the linear velocity, $[p, q, r]$ is the angular velocity, $[F_x, F_y, F_z]$ is the total force exerted on the object and $[T_x, T_y, T_z]$ is the resulting torque. The angles ϕ , θ and ψ are called Euler angles or angles of Tait-Bryan, and provide the orientation of the body, in other words, allow to relate the representations of vectors in the inertial frame with their corresponding representations in the body frame. In particular, the Eq.(4) relates the coordinates of the velocity vector expressed in the body frame ($[u, v, w]$) with the velocity vector expressed in the inertial frame ($[\dot{x}, \dot{y}, \dot{z}]$). Moreover, the Eq.(5) models the evolution of the orientation given by the Euler angles as a function of the angular velocity of the projectile in the body frame ($[p, q, r]$).

Note that from Eq.(4) to Eq.(7) the Euler angles are involved just in the cinematics equations. Therefore, if another representations approach is chosen for the body orientation, for example, utilizing quaternions, the matrix of cosin directors or the rotation vector will change but the general form of the dynamics equations will remain unchanged.

3.1 Quaternions

A quaternion is defined by the expression $\hat{q} = \langle q_e, \mathbf{q}_v \rangle$ where q_e is the scalar part of the quaternion and $\mathbf{q}_v = (q_{v_1}, q_{v_2}, q_{v_3})$ its vector part. Forward, the principal operations that could be performed with a quaternion could be appreciated in [Coutsias and Romero \(2004\)](#).

A very interesting property of the quaternions is that if a quaternion is defined as:

$$\hat{q}_{\alpha, \mathbf{u}} = \langle c_{(\alpha/2)}, \mathbf{u}s_{(\alpha/2)} \rangle, \quad (8)$$

where α is any angle and \mathbf{u} a unit vector, so the result of the operation $\hat{q} \langle 0, \mathbf{v} \rangle \hat{q}^*$, where \mathbf{v} is any vector, it is a quaternion which scalar part is 0 and which vector part correlates with performing a rotation of the vector \mathbf{v} the angle α , having the vector \mathbf{u} as an axis, according with the Right-hand Rule. Also, it could be assessed that any unit quaternion \hat{q} could be expressed as $\langle c_{(\alpha/2)}, \mathbf{u}s_{(\alpha/2)} \rangle$. Therefore, if there is a unit quaternion, the product $\hat{q} \langle 0, \mathbf{v} \rangle \hat{q}^*$ always correlates with a rotation as it was mentioned. So a huge profit could be obtained if the orientation of the object is represented by an unit quaternion \hat{q} by the way of $\langle 0, \mathbf{v}^i \rangle = \hat{q} \langle 0, \mathbf{v}^b \rangle \hat{q}^*$ transform the representation \mathbf{v}^b of each vector \mathbf{v} in the body frame to each representation \mathbf{v}^i in the inertial frame. The Eq.(6) should be replaced by:

$$\langle 0, (\dot{x}, \dot{y}, \dot{z}) \rangle = \hat{q} \langle 0, (u, v, w) \rangle \hat{q}^* \quad (9)$$

Equivalently, the Eq.(9) could be represented in matrix form as:

$$\begin{bmatrix} \dot{x} \\ \dot{y} \\ \dot{z} \end{bmatrix} = Q_b^i \begin{bmatrix} u \\ v \\ w \end{bmatrix}, \quad (10)$$

where

$$Q_b^i = \begin{bmatrix} q_e^2 + q_{v_1}^2 - q_{v_2}^2 - q_{v_3}^2 & 2(q_{v_1}q_{v_2} - q_e q_{v_3}) & 2(q_{v_1}q_{v_3} + q_e q_{v_2}) \\ 2(q_{v_1}q_{v_2} + q_e q_{v_3}) & q_e^2 - q_{v_1}^2 + q_{v_2}^2 - q_{v_3}^2 & 2(q_{v_2}q_{v_3} - q_e q_{v_1}) \\ 2(q_{v_1}q_{v_3} - q_e q_{v_2}) & 2(q_{v_2}q_{v_3} + q_e q_{v_1}) & q_e^2 - q_{v_1}^2 - q_{v_2}^2 + q_{v_3}^2 \end{bmatrix}. \quad (11)$$

Moreover, the Eq.(5) have to be replaced by a expression that relates the evolution of the quaternion with the angular velocity of the projectile. This is coupled by the [Coutsias and Romero \(2004\)](#)

$$\dot{\hat{q}} = \frac{1}{2} \hat{q} \langle 0, (p, q, r) \rangle. \quad (12)$$

As in the Eq.(9), this equation could be defined in a matrix form as:

$$\begin{bmatrix} \dot{q}_e \\ \dot{q}_{v_1} \\ \dot{q}_{v_2} \\ \dot{q}_{v_3} \end{bmatrix} = \frac{1}{2} \begin{bmatrix} -q_{v_1} & -q_{v_2} & -q_{v_3} \\ q_e & -q_{v_3} & q_{v_2} \\ q_3 & q_e & -q_{v_1} \\ -q_{v_2} & q_{v_1} & q_e \end{bmatrix} \begin{bmatrix} p \\ q \\ r \end{bmatrix}. \quad (13)$$

In fact the motion of an object utilizing quaternions for its mathematical representation is defined by the kinematic equations Eq.(14) and Eq.(15), and the dynamics equations Eq.(6) and Eq.(7), which are expressed in the following system, where Q_b^i is described by Ec.(11):

- Cinematics Equations:

$$\begin{bmatrix} \dot{x} \\ \dot{y} \\ \dot{z} \end{bmatrix} = Q_b^i \begin{bmatrix} u \\ v \\ w \end{bmatrix}, \quad (14)$$

$$\begin{bmatrix} \dot{q}_e \\ \dot{q}_{v_1} \\ \dot{q}_{v_2} \\ \dot{q}_{v_3} \end{bmatrix} = \frac{1}{2} \begin{bmatrix} -q_{v_1} & -q_{v_2} & -q_{v_3} \\ q_e & -q_{v_3} & q_{v_2} \\ q_3 & q_e & -q_{v_1} \\ -q_{v_2} & q_{v_1} & q_e \end{bmatrix} \begin{bmatrix} p \\ q \\ r \end{bmatrix}. \quad (15)$$

- Dynamics Equations: This equations remains similar to Ec.(6) and Ec.(7).

3.1.1 Advantages and Disadvantages utilizing quaternions

As a matter of facts, the Eq.(5) exhibits it weakness when the pitch angle (θ) is $\pm\pi/2$, [Pucheta et al. \(2014\)](#). This singularity is known as *gimbal lock*. No matter the sequence in which the rotation is performed corresponding to the Euler's angles, there will always be a singularity for any of the angles involved. Even though, utilizing quaternions does not present any problem of this characteristics. Furthermore, as it shows Eq.(4) and Eq.(5), performing a simulation of a model based on Euler's angles, requires many evaluations of multiple trigonometric functions. Nevertheless, Eq.(14) and Eq.(15) just involves additions and multiplications. This differences hold a huge profit for quaternions when you are working with limited numerical resources or

low requirements on real time. However, while the Euler's angles just required the employ of only three values (θ, ϕ, ψ) for the representation of a body orientation, utilizing quaternions required employing an additional value $(q_e, q_{v1}, q_{v2}, q_{v3})$.

Finally, an additional drawback of utilizing quaternions is that they are not intuitive either when defining orientation references on the tracking algorithms or when observing the behavior of the system. For instance, observing graphs of the temporary evolution of roll, pitch and yaw gives a good idea of the behavior of the system, while observing the graphs of $(q_e, q_{v1}, q_{v2}, q_{v3})$ could not be intuitively understood. Nevertheless, this awkwardness can easily be avoided performing conversions between the two reference systems. First, from the definition of *roll* (ϕ) , *pitch* (θ) and *yaw* (ψ) the corresponding quaternion could be calculated by the product

$$\hat{q}(\phi, \theta, \psi) = \hat{q}_{\psi, k} \hat{q}_{\theta, j} \hat{q}_{\phi, i}, \quad (16)$$

where $\hat{i} = (1; 0; 0)$, $\hat{j} = (0; 1; 0)$ y $\hat{k} = (0; 0; 1)$. On the other hand, the Euler's angles corresponding to the quaternion \hat{q} could be calculated as Bekir (2007)

$$\begin{cases} \phi = \arctan2(q_{v2}q_{v3} + q_e q_{v1}, \frac{1}{2} - (q_{v1}^2 + q_{v2}^2)) \\ \theta = \arcsin(-2(q_{v1}q_{v3} - q_e q_{v2})) \\ \psi = \arctan2(q_{v1}q_{v2} + q_e q_{v3}, \frac{1}{2} - (q_{v2}^2 + q_{v3}^2)) \end{cases}, \quad (17)$$

where $\arctan2(a, b)$ is the angle belonging to the interval $(-\pi, \pi)$ which sin is $\frac{a}{\sqrt{a^2+b^2}}$ and which cosin is $\frac{b}{\sqrt{a^2+b^2}}$. It should be noted that the resulting angles ϕ and ψ will be in the range $(-\pi, \pi)$ and the angle θ in the range $(-\pi/2, \pi/2)$. Therefore, if the Euler's angles are defined out of this range, and the corresponding quaternions are obtained by Ec. (16), and then recovering the Euler's angles by Ec. (17), the resulting angles will not agree with the original angles.

4 ANGULAR MOMENTS ANALYSIS - EULER'S EQUATION APPLICATION

The angular momentum is given by the equation $\vec{M} = \underline{I}\vec{\Omega}$, where the moment vector is proportional to the angular velocity as long as the body is rotating on the principal axes of inertia, which corresponds to situation where the angular velocity is aligned with the moment vector. On the other hand, if the body rotates in any other direction then the angular velocity is not aligned with the moment vector and a movement known as *precession* will occur.

In the following sections different solutions are analyzed for systems in which there are no external efforts, both Forces and Moments. The trajectory described by the body will be given by the temporal evolution of the equations of motion, Eq.(18), which are summarized in the 6ODE's (Ordinary Differential Equations) Landau and Lifshitz (1976). As the core of the research is the rotation, the translation analysis is avoided, studying just rotation. Also, contributions due to external torques are omitted.

$$\begin{cases} \dot{\Omega}_1 = \frac{1}{I_1} \sum T_1^{ext} + \frac{(I_2 - I_3)}{I_1} \Omega_3 \Omega_2 \\ \dot{\Omega}_2 = \frac{1}{I_2} \sum T_2^{ext} + \frac{(I_3 - I_1)}{I_2} \Omega_1 \Omega_3 \\ \dot{\Omega}_3 = \frac{1}{I_3} \sum T_3^{ext} + \frac{(I_1 - I_2)}{I_3} \Omega_2 \Omega_1 \end{cases} \quad \begin{cases} \dot{\Omega}_1 = \frac{(I_2 - I_3)}{I_1} \Omega_3 \Omega_2 \\ \dot{\Omega}_2 = \frac{(I_3 - I_1)}{I_2} \Omega_1 \Omega_3 \\ \dot{\Omega}_3 = \frac{(I_1 - I_2)}{I_3} \Omega_2 \Omega_1 \end{cases} \quad (18)$$

4.1 Spherical Top

In this situation all inertias are identical, $I_1 = I_2 = I_3$, so the solutions for the ODE are constants values depending on the initial conditions, Eq.(19).

$$\begin{cases} \dot{\Omega}_1 = \frac{(I_1-I_1)}{I_1} \Omega_3 \Omega_2 \\ \dot{\Omega}_2 = \frac{(I_1-I_1)}{I_2} \Omega_1 \Omega_3 \\ \dot{\Omega}_3 = \frac{(I_1-I_1)}{I_3} \Omega_2 \Omega_1 \end{cases} \quad \begin{cases} \dot{\Omega}_1 = 0 \\ \dot{\Omega}_2 = 0 \\ \dot{\Omega}_3 = 0 \end{cases} \quad \begin{cases} \Omega_1 = C_1 \\ \Omega_2 = C_2 \\ \Omega_3 = C_3 \end{cases} \quad (19)$$

4.2 Symmetrical top

The symmetrical-top bodies are objects with two similar inertias and the third not, $I_1 = I_2 \neq I_3$. The equality of the inertias is applied, consequently the Eq.(18) turned into Eq.(20).

$$\begin{cases} \dot{\Omega}_1 = \frac{(I_1-I_3)}{I_1} \Omega_3 \Omega_2 \\ \dot{\Omega}_2 = \frac{(I_3-I_1)}{I_1} \Omega_1 \Omega_3 \\ \dot{\Omega}_3 = \frac{(I_1-I_2)}{I_3} \Omega_2 \Omega_1 \end{cases} \quad \begin{cases} \dot{\Omega}_1 = \frac{(I_1-I_3)}{I_1} \Omega_3 \Omega_2 \\ \dot{\Omega}_2 = \frac{(I_3-I_1)}{I_1} \Omega_1 \Omega_3 \\ \dot{\Omega}_3 = \frac{(0)}{I_3} \Omega_2 \Omega_1 \end{cases} \quad \begin{cases} \dot{\Omega}_1 = \frac{(I_1-I_3)}{I_1} \Omega_3 \Omega_2 \\ \dot{\Omega}_2 = \frac{(I_3-I_1)}{I_1} \Omega_1 \Omega_3 \\ \dot{\Omega}_3 = 0 \end{cases} \quad (20)$$

where Ω_3 is a constant value $\Omega_3 = C_1$ and therefore the product of a constant times Ω_3 is also a constant value, which is named w . The term in the equation of Ω_1 will be $-w$ since $(I_1 - I_3) = -(I_3 - I_1)$.

$$\boxed{\begin{matrix} \Omega_{1(t)} = A \cos(w t) \\ \Omega_{2(t)} = A \sin(w t) \end{matrix}} \quad (21)$$

Eq.(21) is the solution of the 2nd order ODE Ec.(20) which models a harmonic motion in two dimensions describing the curved path, where A is the amplitude, and ω the frequency. Strictly speaking, the frequency is $f = \frac{w}{2\pi}$ and ω is the angular velocity of rotation. In other words, the movement described is periodic, since after a while the vector returns to its initial position and the cycle begins again. Hence ω is the speed with which the angular velocity vector $\vec{\Omega}$ changes and therefore the instantaneous axis of rotation. This behavior is known as *precession* phenomenon and is defined as the movement associated with the change of direction in space experienced by the instantaneous axis of rotation of a body, where that speed of change is the precession speed Ω_{pr} . Eq.(22) details this situation.

$$\Omega_{pr} = \tilde{C} \Omega_3 = \overbrace{\left(\frac{I_3 - I_1}{I_1} \right)}^{\tilde{C}} \Omega_3 = \omega \quad (22)$$

In this way, Eq.(22) is reformulated, being now expressed with the precession speed Ω_{pr} .

$$\boxed{\begin{matrix} \Omega_{1(t)} = A \cos(\Omega_{pr} t) \\ \Omega_{2(t)} = A \sin(\Omega_{pr} t) \end{matrix}} \quad (23)$$

Finally from Eq.(23) and Eq.(20) it is concluded that the rotation speed of the body is:

$$\vec{\Omega} = \begin{bmatrix} \Omega_1 \\ \Omega_2 \\ \Omega_3 \end{bmatrix} = \begin{bmatrix} A \cos(\Omega_{pr} t) \\ A \sin(\Omega_{pr} t) \\ C_1 \end{bmatrix} \quad (24)$$

Thus, Eq.(24) presents the general angular velocity of the object. Indeed, $\vec{\Omega} = \vec{\Omega}_{(t)}$ changes instant by instant, hence it is constant with respect to the main axis x_3 but as it is describing a circumference, the vector $\vec{\Omega}$ will follow that path and assuming different values from instant to instant. How fast the vector travels around the circumference is known as precession speed, Ω_{pr} .

4.3 Asymmetrical Top

Now the study is performed for a body where the three moments of inertia are different between each other, that is, $I_1 \neq I_2 \neq I_3$ and also $I_1 > I_2 > I_3$. If the analysis is performed from the conservation of the angular momentum point of view, where $\vec{M} = \underline{I} \vec{\Omega}$ thus if the moment stays constant, $|\vec{M}| = C$, then by increasing $I \uparrow$, results in a decrease of $\Omega \downarrow$. That is I_3 will be the smallest axis of inertia and therefore will have the highest spin velocity.

Eq.(25a) is the equation of the kinetic energy of rotation, which represents all the configurations so that the object has the maximum energy of rotation for certain angular velocities $\vec{\Omega}$. This energy is a scalar magnitude ($E \in CT(0)$ ⁴) and its value is constant during rotation since they are conserved due to the absence of diffusive effects that may vary the energy of the system. Otherwise, Eq.(25b) is the moment equation and is a vector magnitude, $M \in CT(1)$. It should be noted that what is constant is not the momentum but its magnitude. Both Eq.(25a) and Eq.(25b) will remain constant.

$$\begin{cases} E &= \frac{1}{2} [I_1 \Omega_1^2 + I_2 \Omega_2^2 + I_3 \Omega_3^2] \\ |\vec{M}|^2 &= I_1^2 \Omega_1^2 + I_2^2 \Omega_2^2 + I_3^2 \Omega_3^2 \end{cases} \quad (25)$$

The system of equations given by Eq.(25) geometrically represents two ellipsoids, which when compared with the canonical equation of the ellipse, Eq.(26) it is shown that the semi-axes for the energy ellipse, Eq.(25a) are $a = \pm \sqrt{\frac{2E}{I_1}}$, with its analogous for 'b' and 'c', while for the moment ellipse, Eq.(25b), $a = \pm \sqrt{\frac{|\vec{M}|^2}{I_1^2}}$, and its analogous for 'b' and 'c', where the semi-axes correspond to each principal axis of rotation.

$$1 = \frac{x^2}{a^2} + \frac{y^2}{b^2} + \frac{z^2}{c^2} \quad (26)$$

Therefore the system of equations, Eq.(25) expressed in the canonical form of the ellipse, is presented in the form:

$$\begin{cases} 1 &= \frac{\Omega_1^2}{\frac{2E}{I_1}} + \frac{\Omega_2^2}{\frac{2E}{I_2}} + \frac{\Omega_3^2}{\frac{2E}{I_3}} \\ 1 &= \frac{\Omega_1^2}{\frac{|\vec{M}|^2}{I_1^2}} + \frac{\Omega_2^2}{\frac{|\vec{M}|^2}{I_2^2}} + \frac{\Omega_3^2}{\frac{|\vec{M}|^2}{I_3^2}} \end{cases} \quad (27)$$

Solving the intersection of both ellipses involves a considerable complexity. However, if we consider expressing the angular velocity of Eq.(25a) as a function of the moment where

⁴CT refers to a Cartesian Tensor, indicating the range of the tensor. CT (0) is a zero order tensor, that is, a scalar, CT (1) vector, etc.

$M_i = I_{ij}\Omega_j \rightarrow \Omega_j = \frac{M_i}{I_{ij}}$, the same for Eq.(25b), a system related by the moment is obtained, Eq.(29).

$$\begin{cases} E &= \frac{1}{2} [I_1 \Omega_1^2 + I_2 \Omega_2^2 + I_3 \Omega_3^2] \\ E &= \frac{1}{2} \left[I_1 \left(\frac{M_1}{I_1} \right)^2 + I_2 \left(\frac{M_2}{I_2} \right)^2 + I_3 \left(\frac{M_3}{I_3} \right)^2 \right] \\ 2E &= \frac{M_1^2}{I_1} + \frac{M_2^2}{I_2} + \frac{M_3^2}{I_3} \\ 1 &= \frac{M_1^2}{2EI_1} + \frac{M_2^2}{2EI_2} + \frac{M_3^2}{2EI_3} \end{cases} \quad (28)$$

Eq.(28) shows the geometric representation of an ellipsoid with respect to the moment with semi-axes at $a = \sqrt{2EI_1}$, and its analogous for ' b 'and' c '. Where, as it was said before, the ellipsoid represents the configurations of the system where the maximum energy of rotation is obtained, and the semi-axes are the principal axes of inertia.

$$\begin{cases} 1 &= \frac{M_1^2}{2EI_1} + \frac{M_2^2}{2EI_2} + \frac{M_3^2}{2EI_3} \\ |M|^2 &= M_1^2 + M_2^2 + M_3^2 \end{cases} \quad (29)$$

Therefore, with the transformation, a system of equations expressed in terms of the the angular momentum is achieved, Eq.(29). This system consists in the energy of rotation and the angular momentum. Geometrically, the solution of the system represents the intersection between an ellipsoid and a sphere, which is simpler and more intuitive solution rather than two ellipsoids. This expression shows that the moment will have two bounded values by the semi-axes of the energy ellipsoid, that is, all the admissible solutions that are between the minimum and maximum value of the semi-axes, Eq.(30).

For a better comprehension an algorithm was developed in *GNU-Octave* software where the intersection of an sphere and a ellipsoid was solved. This situation is presented in Fig.(1) where all the possible solutions for the intersection between an ellipsoid and a sphere are shown, whose physical analogy would be the rotating configuration assumed by the object for a given moment obtaining the maximum kinetic energy available.

$$\begin{aligned} c^2 &< M^2 < a^2 \\ 2EI_3 &< M^2 < 2EI_1 \end{aligned} \quad (30)$$

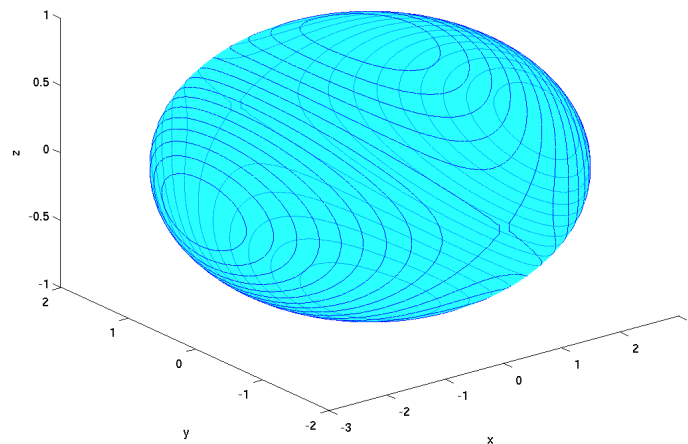


Figure 1: Ellipsoid - Sphere Intersections

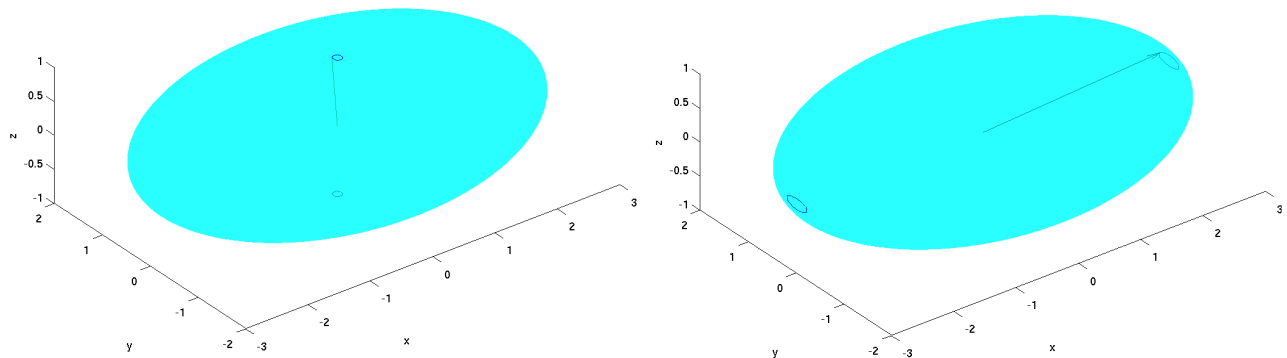


Figure 2: Stable configuration, Moment Path Inertia, I_3 and I_1

4.4 Possible scenarios

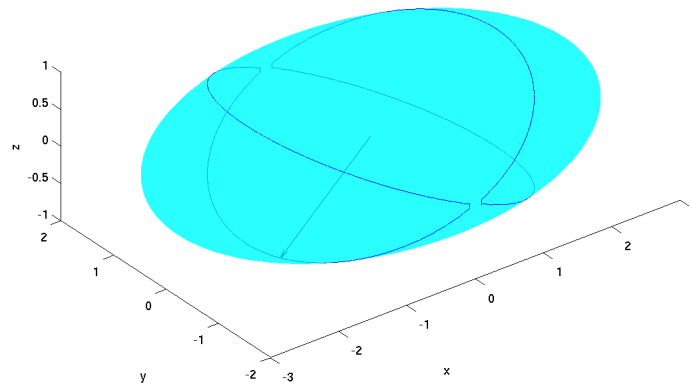
From the system of Eq.(29) for a constant amount of energy there are different possible situations, mainly defined by the three semi-axes, which precisely correspond to the principal axes of inertia, Fig.(1). Furthermore, the possible solutions are analyzed, starting from the minimum value up to the maximum value that the moment can adopt, that is $c^2 < M^2 < a^2$.

To begin with, when the body is rotating about its smallest principal axis of inertia $2EI_3$, this principal axis is collinear with its angular velocity $|\vec{\Omega}|$, and is proportional to the $|\vec{M}|$, this is because the moment vector is aligned with the angular velocity.

However, if the moment has a component that interrupts the collinearity, that is, $|\vec{M}|$ suffers a minimum variation with respect to the axis of inertia, Fig.(2a), in this case the solution of the energy-moment system will be two closed curves. These curves are the solution of the intersection between the energy ellipsoid and the moment sphere; one curve for each side of the ellipsoid. Then, the moment vector $|\vec{M}|$ while moving along the curve performs a cone-shaped movement. This phenomenon is known as *precession* and it is defined as the movement associated with the change of direction experienced by the instantaneous axis of rotation. In other words, it is a parameter that indicates how not-aligned the moment vector $|\vec{M}|$ and the principal axes of inertia are. Although in Sec.(4.2) the mathematical analysis of the precession phenomenon is performed for a *symmetrical-top* body, the same phenomenon also happens in *asymmetrical-top* when the object suffers a variation in the moment \vec{M} close to the smallest axis of inertia⁵.

As the not-alignment increases, the opening degree of the cone will be greater, since the circumference given by the intersection between the ellipsoid and the sphere increases. In this case, the vector \vec{M} will suffer a modification in its components. Although, its magnitude is constant $|\vec{M}| = C_1$, where $C_1 \in CT(0)$, it should be noted the vector component will be modified $\vec{M} = \vec{M}_1 + \vec{M}_2 + \vec{M}_3$. Consequently, the projection on the principal axis of inertia will be smaller and therefore the body will suffer a decrease in its angular velocity, while its difference will contribute to the precession movement, performing a more pronounced circular curve. These situations can be deduced from Fig.(2a) and Fig.(2b).

⁵From development it is manifested that the precession phenomenon occurs both for the smallest axis of inertia I_3 and for the largest I_1

Figure 3: Moment path - Inertia I_2

The graphical interpretation of the *precession* phenomenon is appreciated when the circumference given by the intersection between the ellipsoid and the sphere begins to grow and therefore the projection of the vector moment \vec{M} on the axis of inertia begins to decrease. In other words, the more aligned the vector $|\vec{M}|$ is with respect to the axis of rotation, the greater will be its projection on it, and therefore greater will be its rotation speed $|\vec{\Omega}|$. Since the intersection between the ellipse and the sphere is a closed curve, it is evident that the motion of the moment vector $|\vec{M}|$ is periodic, that is, the vector moves along the path described by the intersection curve and then returns to its original position.

This situation in which a slightly difference of the moment vector $|\vec{M}|$ produces a deviation movement close to the curve, occurs both in the greatest (I_1) and least (I_3) semi-axes of the ellipsoid, Fig.(2). However, it is observed that the situation on the region close to the intermediate axis (I_2), the curve described is different from a circle close to the axis of inertia, Fig.(3). In the case in which the body is rotating about the intermediate axis of inertia (I_2) and experiences a slight variation on the moment $|\vec{M}|$, it will have a qualitative different behavior, where the moment vector $|\vec{M}|$ performs a totally strange and away path from the "poles" of the semi-axis.

This situation is due to the fact that the rotational movement of the body about the greatest (I_1) and least (I_3) semi-axes are stable, while the rotational movement with respect to the intermediate axis (I_2) is unstable, generating that strange and amazing disturbance described during the rotation about the 2^{nd} principal axis. This phenomenon is known as the paradox of the tennis racket or the intermediate axis theorem, also known as the 'Dzhanibekov' effect or the Wingnut effect, and graphically it is manifested that this bizarre trajectory is due to the intersection between the ellipsoid and the sphere that occurs close to the second principal axis of inertia, Fig.(3).

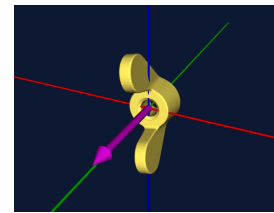
5 METHODOLOGY

To deal with technical issues, an algorithm that solves the RBD model with 6DOF's was developed and it uses quaternions for the mathematical representation of the body's orientation. This is an advantage since such modeling allows representing displacements in any direction, an issue that is not possible if Euler's angles are used due to the singularity known as *gimbal-lock*.

The algorithm solves the Euler's law of motion equations, Eq.(18) and models the trajectory of a body under the initial conditions of motion. It is implemented in Python language and in order to solve the ODE's, a temporal integrator with an adaptive time step is used. It is supplied

	Descripción		Descripción
masa	0.1 [kg]	diam	0.04 [m]
I_{XX}	1.3442e-8	x_{CG}	0
I_{YY}	1.6312e-8	y_{CG}	0
I_{ZZ}	5.4941e-9	z_{CG}	0

(a) Wingnut's Characteristics



(b) Wingnut's Axiometry

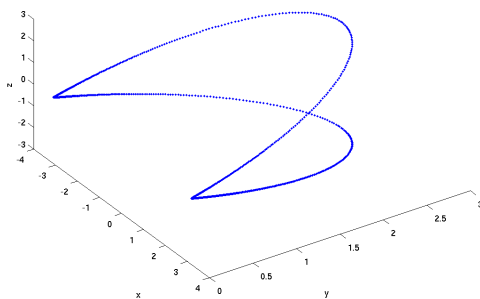
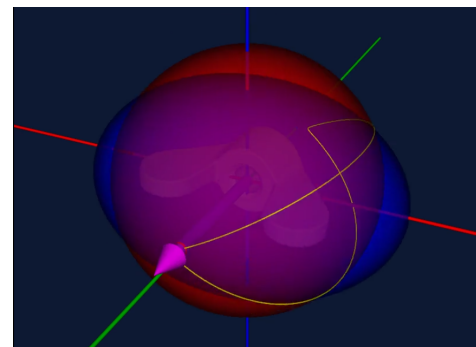
Figure 4: Asymmetrical-top Object

by the physical parameters of the object, such as its geometric parameters, inertia, center of mass, etc. The model returns as a result the numerical values of the trajectory and graphs that show the evolution of the parameters involved.

6 RESULTS

6.1 Numerical Simulations

Several numerical simulations are performed on which translations are omitted since these values do not affect the effects of rotation. The selected object was an *asymmetrical-top* wingnut with the characters shown in Fig.(4). Fig.(5a) shows the path performed by the Moment vector \vec{M} which indeed agrees with the instability analysis performed in Sec.(4.4).

(a) Moment path, \vec{M} 

(b) Wingnut Result

Figure 5: RBD Result, rotation over intermediate axis

6.2 Rotation sequence, intermediate axis instability

Fig.(6) shows the rotations sequence of the instability experienced by a *asymmetrical-top* body when it rotates about its intermediate axis. For a better understanding, the rotation is represented meantime the different parameters involved are placed, such as: the energy ellipsoid, the moment sphere, the moment vector and also the trajectory that the moment describes. The magenta vector represents the moment vector, \vec{M} , which at all times follows the path given by the intersection between the energy ellipsoid and the moment sphere. For a better visual understanding, the energy ellipsoid is represented in blue, while the moment sphere is in red. It is shown that the intersection between the two curves (ellipsoid-sphere) is the trajectory described in Fig.(5).

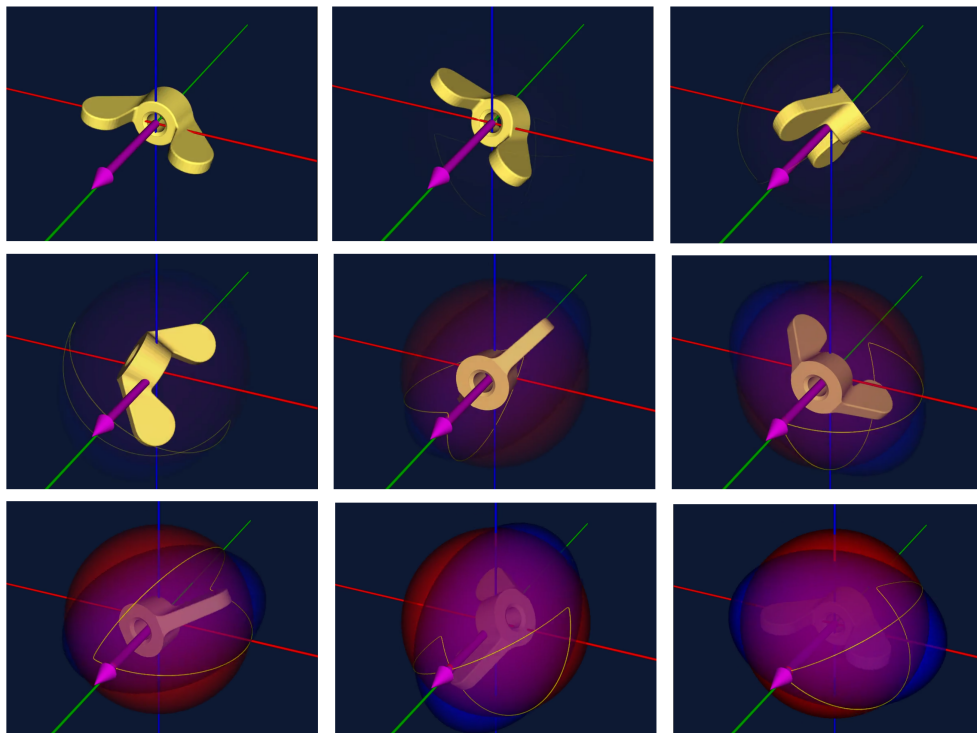


Figure 6: Rotation sequence, intermediate axis instability also known as Dzhanibekov effect

7 CONCLUSIONS

An algorithm that models the RBD (Rigid Body Dynamics) was developed. On this model, the rotations of an object about its three axes of inertia were analyzed. It is shown that for an *asymmetrical-top* object, rotations about the 1st and 3rd axis of inertia are stable. However, rotations about the intermediate axis of inertia present a disturbance that produce a deviation that cause a motion far from the original path. This is due to the fact that rotations about the 2nd axis of inertia are unstable. This phenomenon is known as intermediate axis instability, tennis racket paradox or 'Dzhanibekov' effect. The solution of the ODE's system is obtained by a geometric approach, thus obtaining an alternative strategy when analyzing stability of differential equations.

REFERENCES

- Ashbaugh M.S., Chicone C.C., and Cushman R.H. The twisting tennis racket. *Journal of Dynamics and differential Equations*, 3(1):67–85, 1991.
- Bekir E. *Introduction to modern navigation systems*. World Scientific, 2007.
- Coutsias E.A. and Romero L. The quaternions with an application to rigid body dynamics. 2004.
- Kokes J., Costello M., and Sahu J. Generating an aerodynamic model for projectile flight simulation using unsteady time accurate computational fluid dynamic results. *Computational Ballistics III*, 45:11131, 2007.
- Landau L.D. and Lifshitz E.M. *Mechanics: Volume 1*, volume 1. Butterworth-Heinemann, 1976.
- Poinsot L. *Théorie nouvelle de la rotation des corps*. Bachelier, 1851.
- Pucheta M., Paz C.J., and Pereyra M.E. Representaciones cinemáticas de orientación y ecuaciones de estimación. *Mecánica Computacional*, 33(36):2303–2324, 2014.